CONVERSION OF SMECTITE TO AMMONIUM ILLITE IN THE HYDROTHERMAL SYSTEM OF HARGHITA BĂI, ROMANIA: SEM AND TEM INVESTIGATIONS

IULIU BOBOS[1*] and LUCRETIA GHERGARI[2]

[1]Laboratory of Mineralogy, Polytechnic University of Timisoara, Timisoara-1900, Romania
[2]Department of Mineralogy, "Babes-Bolyai" University, Cluj Napoca-3400, Romania

Abstract: Random and ordered mixed-layer smectite-ammonium illite (NH_4-I/S) were identified by XRD analysis in the fossil hydrothermal system of Harghita Băi (Eastern Carpathians, Romania). Morphologies of NH_4-I/S were studied by SEM and TEM. SEM image of random NH_4-I/S displays a cellular or cornflake texture. Ordered NH_4-I/S (R=1) exhibits a scalloped morphology with curled edges. Ribbon crystals of illite rise from the surfaces of plate aggregates. Two generations of NH_4-I are distinguished: one developed from a smectite precursor and another from a kaolinite precursor. Hairy illite and illite pseudomorphs after book-like aggregates of kaolinite are present. TEM images show the evolution of morphology from flake to lath habit during the smectite to illite conversion. Particles with veil characteristics and flake particles are observed in random mixed-layered NH_4-I/S. Diffuse lath shaped illite developed on the previous morphology in the expandability range 70–20 %S is observed. Euhedral lath shaped illite is present in NH_4-I/S, below 10 %S. The reaction of smectite-to-illite is continuous, leading to lath shaped illite.

Key words: Eastern Carpathians, Harghita Băi area, XRD, SEM, TEM, random and ordered NH_4-illite/smectite.

Introduction

The reaction of smectite into illite during the diagenetic, metamorphic and hydrothermal processes has been described over more than 25 years by several authors (Perry & Hower 1970; Hower et al. 1976; Boles & Franks 1979; Nadeau & Reynolds 1981; Inoue 1986; Inoue et al. 1987, 1988, 1990; Buatier et al. 1992; Šucha et al. 1993, 1996; Christidis 1995). During the conversion of smectite to illite, the proportion of illite layers and K or NH_4 contents increase with temperature and geological time. Typically, K is the interlayer cation fixed in illite structure, however NH_4 can play an analogical role.

Detailed investigations by SEM and TEM of random and ordered mixed-layer illite/smectite have been made by Nadeau et al. (1985), Inoue (1986), Inoue et al. (1987), Keller et al. (1986), Yau et al. (1987), Christidis (1995), Šucha et al. (1996). Their conclusion concerning the mechanism of smectite to illite conversion is that of dissolution–crystallization.

Amouric & Olives (1991), studying the illite/smectite samples described by Inoue et al. (1987), have shown that both mechanisms of dissolution–crystallization and solid state transformation are involved at the same time in the process of illitization of smectite.

An experimental study of the changes in particle morphology during illitization of smectite was made by Whitney & Velde (1993). They found that this reaction followed four steps: dissolution, epitaxial nucleation and growth of illite on smectite substrata, coalescence of thin illite particles to form aggregates and infillings, and syntaxial growth of aggregates.

However, the understanding of the mechanism of this reaction is limited. No single model can explain the transition of smectite to illite. On the basis of published data, Moore &

Reynolds (1989) quoted four reported genetic models to explain this reaction: the MacEwan crystallite model, the fundamental particle model, the segregated model and two solid solution models.

A complete transition from smectite to ammonium-illite (NH_4-I) has never been reported in the literature. However, some ordered mixed-layer NH_4-illite/smectite (NH_4-I/S) formed during diagenesis, have been described by Copper & Abedin (1981).

Hydrothermal occurrences of NH_4-I or/and mica are known in Slovakia, Japan and the U.S.A. Ammonium sericite was identified by Kozač et al. (1977) in the Neogene Volcanism of Slovak Carpathians (Vihorlat Mts.). In the Japanese volcanic arc, Higashi (1978, 1982) reported NH_4-I as a new mineral named "tobelite" (after Tobe mine). Also, Kawano & Tomita (1988) described ammonium-bearing dioctahedral $2M_1$ mica from Aira district. Wilson et al. (1992) characterized hydrothermal "tobelitic" material, ordered mixed-layer NH_4-I/S, 2–8 % expandable layers (%S), which occur in hydrothermally altered black shale from the Oquirrh Mts. (Utah, U.S.A.).

In this contribution, morphological characteristics of random and ordered mixed-layer NH_4-I/S and the evolution of smectite into illite in the Harghita Băi hydrothermal area (Neogene volcanism of Eastern Carpathians, Romania) were studied by scanning electron microscopy (SEM) and transmission electron microscopy (TEM).

Geological background

The Neogene volcanic activity in the Eastern Carpathians represents a subsequent stage of the magmatism associated

**Present address: Department of Geosciences, University of Aveiro, Aveiro-3810, Portugal

with the Carpathian orogen. The Călimani–Gurghiu–Harghita volcanic arc is the youngest unit of the Carpathians and it developed in two stages, represented by two structural compartments: lower volcanoclastic and upper stratovolcanic (Fig. 1). The volcanic edifice of Harghita Băi situated in a craterial join of a stratovolcano, developed during two main stages: stratovolcanic and intrusive.

An intrusive microdiorite and andesite formation (upper Pliocene) succeeds a variety of andesitic rocks developed
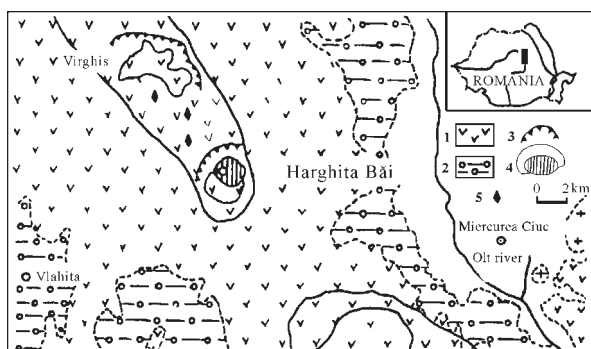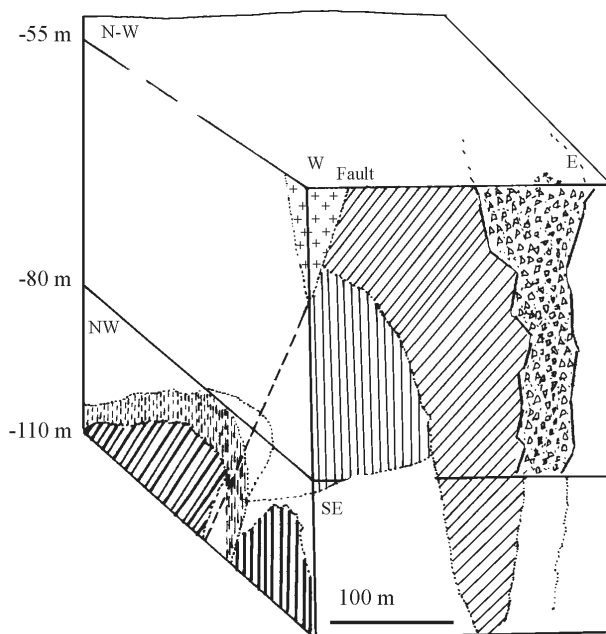

Fig. 1. Geological sketch of central area of Harghita Mts.: **1** — upper structural compartment; **2** — lower structural compartment; **3** — craterial area; **4** — argillization area; **5** — centre of eruptions.

LEGEND
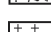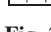
- NH_4-illite/smectite (R3) assemblage
- NH_4-illite/smectite (R1;R2) assemblage
- K-illite/smectite (R3) assemblage
- smectite assemblage
- chlorite/smectite assemblage
- explosion breccia ("breccia pipe")
- intrusive dyke

Fig. 2. The location of mixed-layer NH_4-I/S and NH_4-I in the breccia pipe structure.

closer to the surface. The hydrothermal alteration of Harghita Băi is related to the evolution of a porphyry copper system and it is characterized by the following stages: biotitic, amphibolic, chloritic and argillic (Stanciu 1984).

The fragment of the hydrothermal area investigated by Bobos (1994) in the mining works from 0 to –110 meters below the present surface is characterized by two types of alteration: an advanced argillic alteration (kaolinite ± dickite ± pyrophyllite assemblage and sudoite + Na-rectorite ± K-illite assemblage), interpreted as a "satellite" alteration of the porphyry copper system, and a late alteration enriched in NH_4-I related to the breccia pipe structures (BPS). NH_4-I alteration is superimposed on the porphyry copper system. The late alteration took place after the change of the fluid regime from lithostatic to hydrostatic, which yielded hydraulic fracturing expressed by BPS (Bobos 1994). The BPS are devoid of ore minerals and are composed of irregular polygonal blocks of argillized pyroxene andesite enriched in NH_4-I. The postmagmatic event related to the BPS is supposed to be associated with residual hydrothermal fluids enriched in nitrogen and boron. The spatial relationship between the BPS and the alteration zones enriched in ammonium is shown in Fig. 2.

Materials and methods

Both random and ordered mixed-layer NH_4-I/S, as well as NH_4-I, occur in the Harghita Băi hydrothermal area. Samples containing random mixed-layer NH_4-I/S are mixtures containing small amounts of other clay minerals (kaolinite and chlorite) and occur outside the BPS at depths of –110 meters. Ordered mixed-layer NH_4-I/S (10 to 40 %S) come from the external part of the BPS and were collected at the depth range of –50 to –110 meters.

The < 2 μm fractions were separated by sedimentation and treated by Jackson's (1975) technique. X-ray diffraction (XRD) patterns were recorded for oriented specimens, prepared by pipetting clay suspensions of < 2 μm fractions onto glass slides (concentration of 10 mg/cm^2). The saturation with ethylene glycol for the expandability measurement was carried out over 8 hours at 60 °C.

XRD analysis was carried out with a Philips PW-1730 automated system using a Cu, Kα radiation and a graphite monochromator. Samples were analysed in the range 2 to 50° 2θ, using 0.5° divergence and 1° receiving slits, 0.02° 2θ step and counting time of 1sec/step. The expandability of NH_4-I/S and the ordering type (Reichweite) were determined using the methods of Środoń (1980) and Watanabe (1988). The accuracy of %S measurements by both methods is approximately ± 5 %S.

For SEM observations the rocks were crushed into small pieces and then cleaned by ultrasonics. Samples were mounted on a carbon holder. Analysis was carried out with a Jeol-35 scanning electron microscope operated at 15 kV and 25 kV.

For TEM analysis, the < 2 μm fractions were dispersed in water, using an ultrasonic vibrator. Very dilute drops were deposited over copper microgrids covered with a Formvar film. Laurylamine was intercalated in sample HB-1 (NH_4-I/S; R = 0) to prevent the collapse of smectite layers under high vacuum (Murakami et al. 1993). Investigation was performed
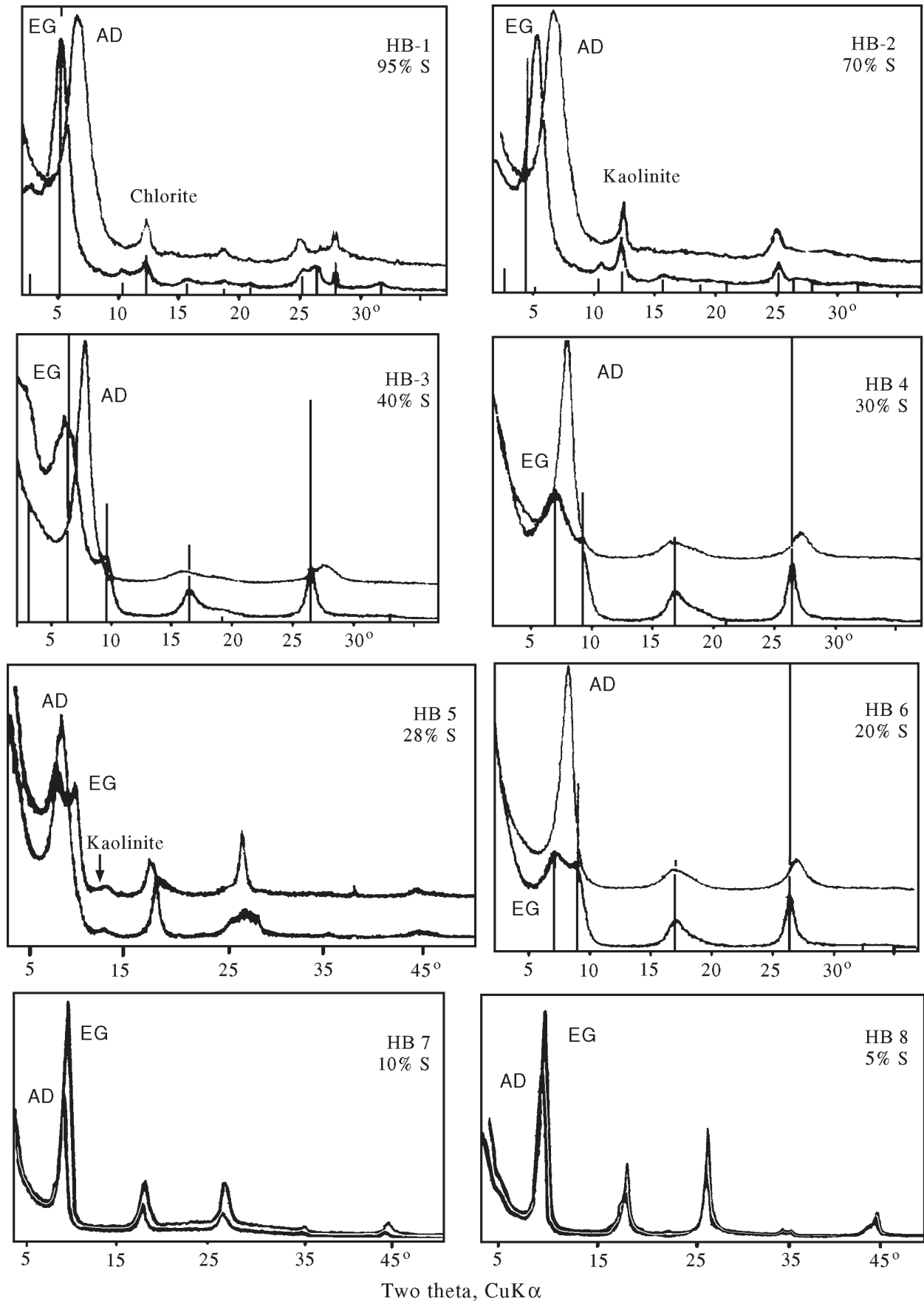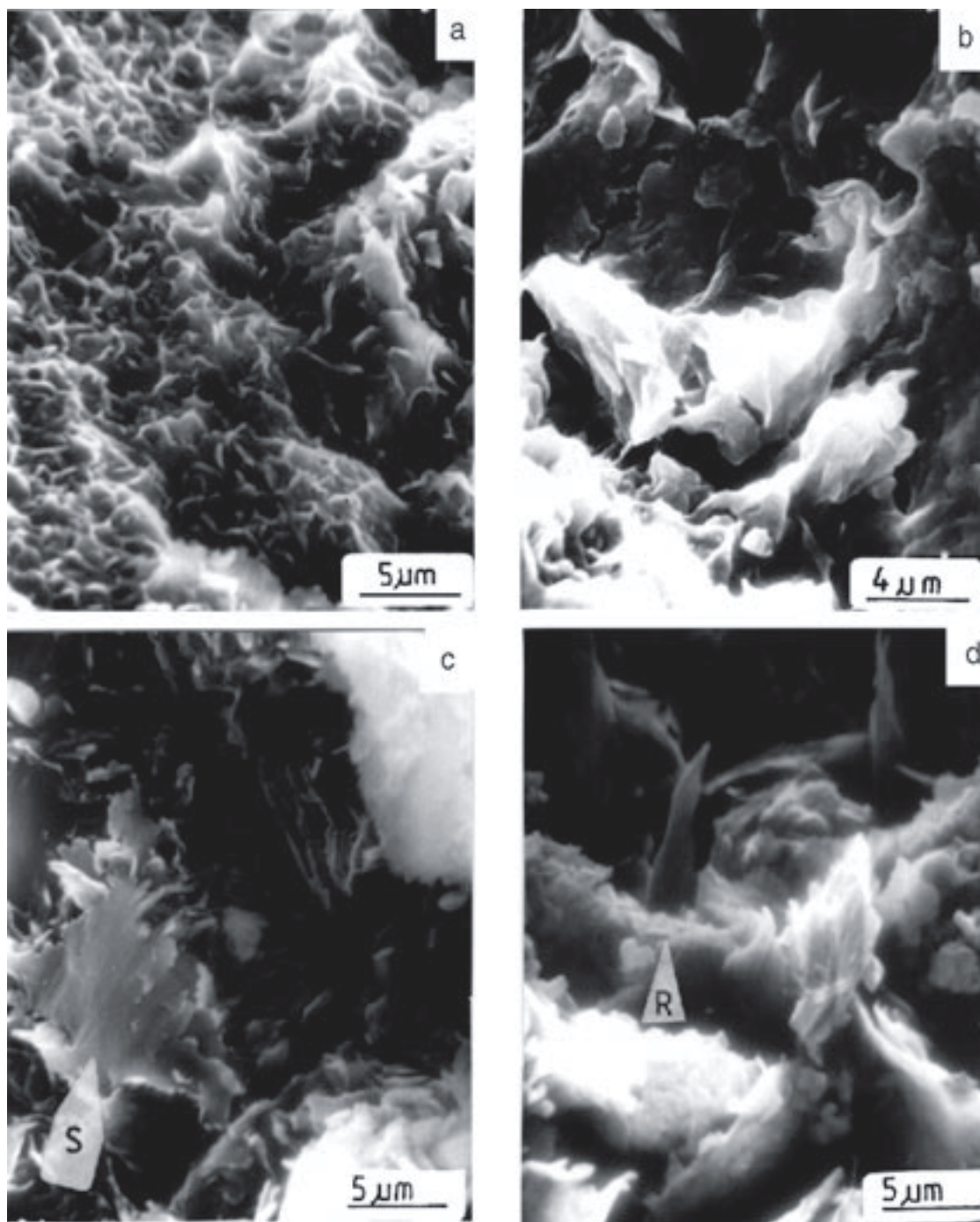
Fig. 3. XRD patterns (air dry and ethylene glycol) of random and ordered mixed-layer NH_4-I/S.

Fig. 4. Text on the next page.

using a Tesla B-500 and a Hitachi H-9000 transmission electron microscopes, both operated at 80 kV.

Results

X-ray diffraction

XRD patterns of random and ordered NH_4-I/S were recorded in air-dry and ethylene glycol states (Fig. 3). The measured expandability is listed in Table 1. The samples with random NH_4-I/S are mixtures with chlorite or kaolinite. Most samples with ordered NH_4-I/S do not contain other minerals in the < 2 µm fractions. Only in the sample HB-6 was a small quantity of kaolinite detected.

NH_4-I/S enriched in ammonium (HB-7; 10 %S) shows the d(005) reflection at 2.05 Å in XRD traces. The XRD patterns of sample HB-8 (5 %S) show two distinct d(005) reflections, both in air-dry and ethylene glycol states: a small shoulder at 2.03 Å corresponding to NH_4-I/S and the reflection at 2.01 Å corresponding to K-I/S. The two peaks were assigned to two separate phases of K-I/S and NH_4-I/S. This is consistent with
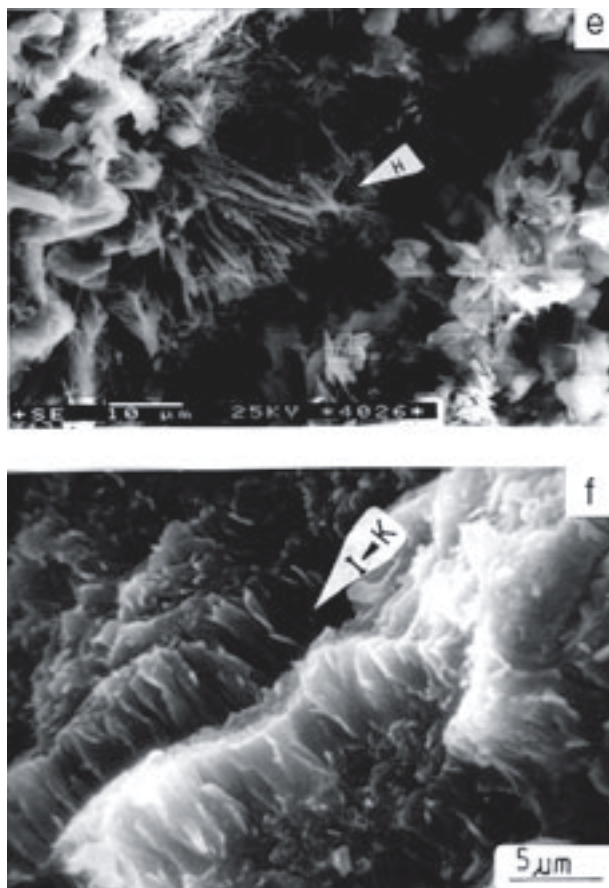
Fig. 4. SEM images: **a** — smectite exhibits a cornflake texture (sample HB-1, 95 %S); **b** — random NH$_4$-I/S (HB-2, 70 %S) showing flat lying flakes; **c** — on the edge of scalloped (S) morphology are present thin flat or ribbon crystals of NH$_4$-illite rising from smectite (HB-3, 40 %S); **d** — ribbon (R) crystal of NH$_4$-illite (HB-4, 30 %S); **e** — hair-like (H) and plate morphology of illite in the sample of K-I/S + NH$_4$-I/S (HB-8, 5 %S); **f** — pseudomorphose of NH$_4$-illite after a kaolinite "book" (HB-7, 10 %S).

Table 1: Location of samples (depth below surface) and XRD characteristics of the NH$_4$-I/S investigated from the < 2 μm fractions.

Samples	Depth	Expandability and Reichweite	Mineral admixtures
HB-1	-110 m	95±5%; R=0	chlorite
HB-2	-55 m	70±5%; R=0	kaolinite
HB-3	-80 m	40±5%; R=1	–
HB-4	-60 m	30±5%; R=1	–
HB-5	-72 m	28±5%; R=1	kaolinite
HB-6	-55 m	20±5%; R=1/R=2	–
HB-7	-60 m	10±5%; R=3	–
HB-8	-88 m	5±5%; R=3	–

the chemical composition of this sample, which showed an increase of K and a decrease of NH$_4$ content, as compared to sample HB-8 (Bobos et al. 1995).

Scanning electron microscopy

SEM images of random mixed-layer NH$_4$-I/S containing 95 %S exhibit a cellular morphology. The flakes of smectite with sharp edges having the typical cornflake texture of montmorillonite, could be seen (Fig. 4a, sample HB-1). With the decrease of expandability, the texture changes and a large number of flat lying flakes is observed (Fig. 4b, sample HB-2; 70 %S). The clay texture in sample HB-3 (40 %S) is dominated by flakes with a scalloped morphology, apparently platy crystals (Fig. 4c). The coalescence of thin flat or ribbon illite is observed. This type of morphology coexists with the digitated texture, where ribbons of illite are arranged like the fingers of a hand. Below 30 %S, further changes in morphology are well evidenced. Elongated "ribbon" illite crystals growing from flakes or scalloped crystals are shown in Fig. 4d (sample HB-5). Ordered NH$_4$-I/S, below 10 %S exhibits a lath morphology. Illite with a hair texture (Fig. 4e) was identified in sample HB-8 of K-I/S + NH$_4$-I/S (5 %S). The length of the hairy illite is more than 10 μm and they are very thin. The hair-like morphology coexists with euhedral quartz. Similar paragenesis (hairy K-I/S and euhedral quartz) was reported from the Shinzan hydrothermal area (Japan) by Inoue (1986). The hair illite morphology does not occur in samples of ammonium clays. NH$_4$-I also formed from kaolinite precursor minerals, is well observed in an illite pseudomorph after "books" of kaolinite (Fig. 4f, sample HB-7).

Transmission electron microscopy

Extremely thin particles of pure smectite are shown in Fig. 5a, (sample HB-1). Individual aggregates have a dominant flake-like habit and curling edges (cornflake texture). Flake-like morphology is also well defined in random mixed-layer NH$_4$-I/S with 70 %S (sample HB-2) and the first thin lath illite particles grown of smectite aggregates were observed (Fig. 5b). Randomly organized laths on a core particle of smectite can be seen. With the decrease of expandability, the flake morphology will gradually disappear. Partially ordered NH$_4$-I/S (40 %S to 30 %S, HB-3 and HB-4) display illite crystals with a lath-like habit, growing on a smectite support (Figs. 5c and 5d). The lath crystal broadens towards the smectite flake.

Morphological investigations of NH$_4$-I/S (R = 1) evidence laths and short fibres developed on smectite along one or more preferential directions with a variable angle of 40° to 60° between them. With the decrease of expandability, the smectite morphology decreases (Fig. 5e; HB-6). It disappears in NH$_4$-I/S below 20 %S. Ordered mixed-layer NH$_4$-I/S, having below 10 %S, display mainly a lath morphology elongated along the a^* direction without flake-like habits (Fig. 5f, sample HB-7; 10 %S). The lath illite correspond to 1M polytype (Güven 1974). In Fig. 5g (sample HB-7) two generations of illite can be distinguished. Lath particles of illite show straight and pseudo-hexagonal edges. These indications of crystal habit can constitute the genetical features for illite formed from smectite and from kaolinite precursor minerals.

Discussion

The smectite to illite reaction via mixed-layer I/S clay minerals has been interpreted in the literature as a solid state transformation or a neoformation process. Solid state transforma-

tion is imagined as alteration of smectite crystals into illite crystals due to Al^{3+} substitution for Si^{4+} and K^+ fixation (Hower et al. 1976). The neoformation process consists of dissolution of smectite and crystallization and growth of illite (Nadeau et al. 1985; Eberl & Środoń 1988; Inoue et al. 1988).

The reaction's progress is influenced by the chemistry of fluids, porosity and permeability, with water playing the main role in the dissolution of smectite and the crystallization of illite (Whitney 1990). Thin illite particles grow and coalesce with increasing temperature and time (Eberl & Środoń 1988). According to Jiang & Peacor (1990), the smectite to illite transition involves only metastable phases controlled by kinetic factors.

In experimental hydrothermal conditions, Whitney (1990) demonstrated that original smectite layers disappeared at 50 %S and then, the first thin illite layers were constituted. Normally, dissolution of smectite is considered to be very fast (Eberl et al. 1986) and take place in randomly mixed-layer I/S.

The first lath illite crystals, coexisting with flake smectite, were observed by Inoue et al. (1987, 1988) and Christidis (1995) at 80–70 %S. Thus, fast dissolution of smectite is reported in their results. In contrast, in ordered NH_4-I/S (R = 1, > 20 %S) the morphology of original smectite (Figs. 5c, 5d, 5e) persists and it tends to disappear only in NH_4-I/S, having less than 20 %S. Illite crystals are oriented at 120° and at 60°–40° angles on smectite aggregates of NH_4-I/S (70 %– 20 %S), suggesting crystal growth and epitaxial coalescence. In fact, in the expandability range 70–20 %S there is a progressive evolution from flake smectite to lath illite, where syntaxial illite grown on smectite is clearly evidenced. According to Whitney & Velde (1993), syntaxial lateral growth of secondary illite layers on primary smectite could appear during the illitization of smectite.

Two types of processes (dissolution–precipitation) may be either the topotactic replacement, where the original smectite or both minerals, smectite and illite are maintained, but may produce overgrowths and growth of new crystals (Whitney & Northrop 1988). Lath shape NH_4-I grown on smectite, can be considered as individual particles which would become increasingly inter-grown or can be interpreted, as aggregates of inseparable units formed of smectite and illite. Layers of illite and smectite are pictured as intimately interlayer (Altaner & Bethke 1988) and the MacEwan model may be a support in the case of random and ordered NH_4-I/S.

Two cases are involved to explain the morphologies of NH_4-I/S, characterized by the coexistence of flaky smectite and lath illite:

1. The fluid flow rate in the smectitic environment was insufficient for an extensive dissolution and leaching, developing the porosity around the smectite flakes. The subsequent reaction was characterized by slow dissolution of smectite and epitaxial growth of illite on smectite surface by topotaxy. Pore chemistry inhibited the smectite to illite reaction;

2. The presence of Na, Ca and Mg interlayer ions are known to inhibit the illitization process of smectite.

The dissolution of smectite is related to water in the geological system. Water with a catalyst role is important for transport and crystallization, although, a small amount of water can slow the dissolution of smectite and enhance extensive substitution of the smectite through illite. The reaction of smectite illitization was inhibited due to the deficit of water in the system and therefore, it was controlled by the porosity. A complete illitization process of both smectite and kaolinite is nevertheless attested in the BPS through NH_4-I clays.

Taking into account the second case, the presence of Mg^{2+} ions in the solution will retard the rate of illitization. The chemistry of ordered mixed layer NH_4-I/S (40 to 20 %S), shows values of the Mg content in the range 0.31–0.41/ $O_{10}(OH)_2$ (Bobos et al. 1995). As a matter of fact, Roberson & Lahann (1981) demonstrated in experimental conditions the role of Na^+, Ca^{2+} and Mg^{2+} in the pore fluids during the smectite to illite conversion.

Therefore both stages are involved in the illitization of smectite from the Harghita Băi area and can explain the long rate of smectite dissolution. The availability of NH_4 influenced more or less the low rate of the reaction. No other byproduct was identified in the clay fractions of the BPS. On the contrary, kaolinite chlorite, quartz and cristobalite associated with NH_4-I/S were identified outside the BPS. The NH_4 availability was sufficiently in the main channel and the smectite and kaolinite were consumed, leading to illite layers.
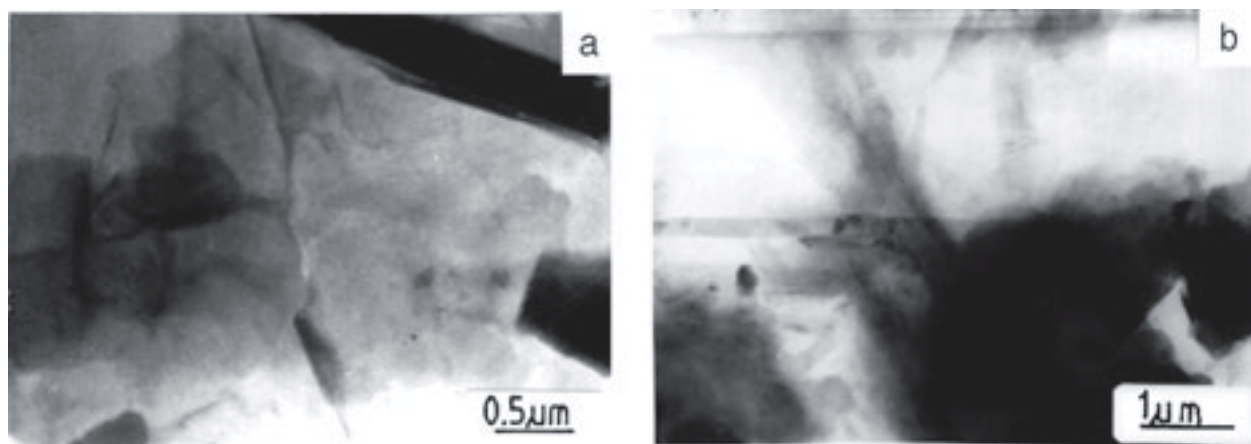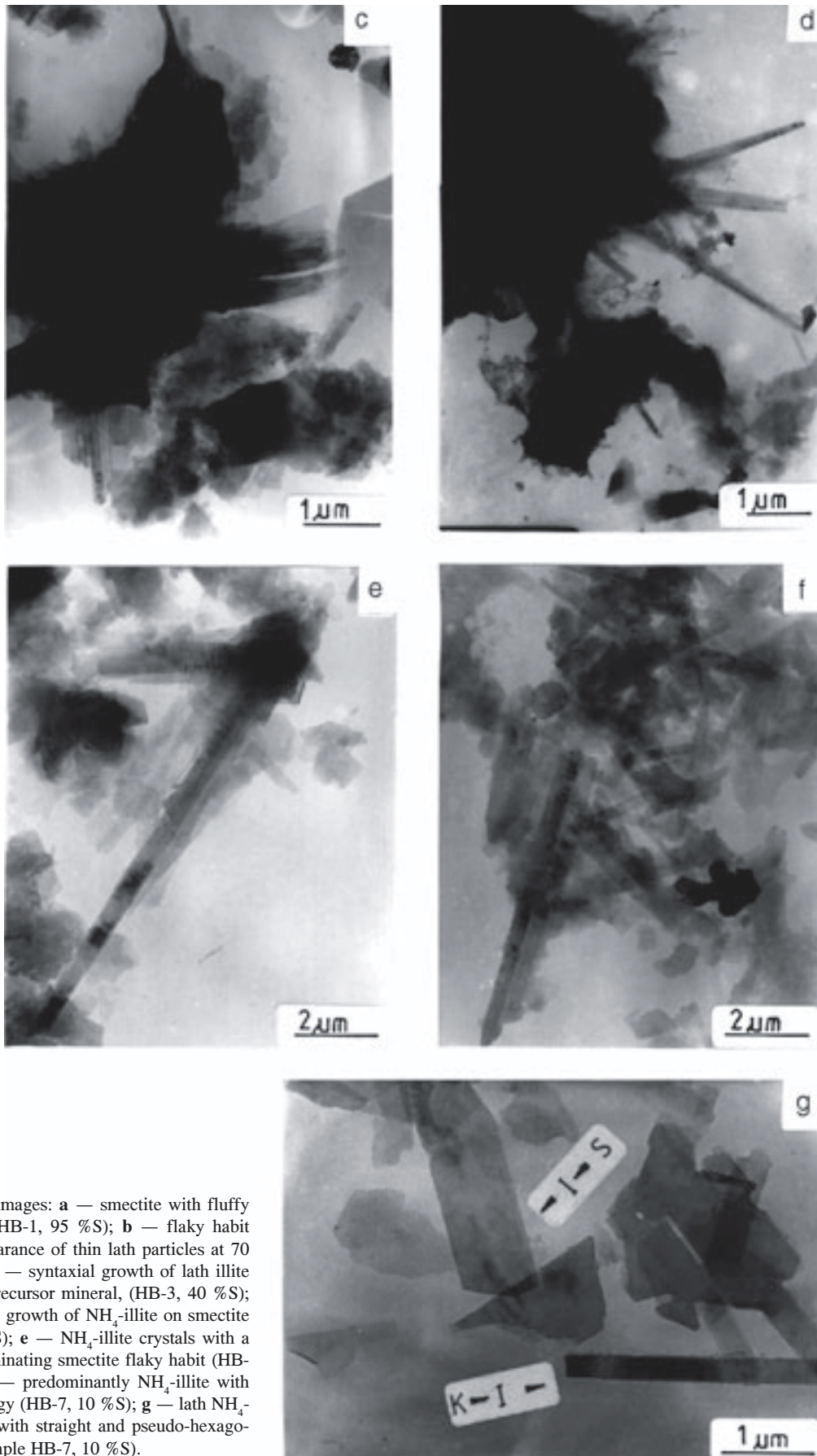

Fig. 5. Text on the next page.

Fig. 5. TEM images: **a** — smectite with fluffy morphology (HB-1, 95 %S); **b** — flaky habit and first appearance of thin lath particles at 70 %S (HB-2); **c** — syntaxial growth of lath illite on smectite precursor mineral, (HB-3, 40 %S); **d** — syntaxial growth of NH$_4$-illite on smectite (HB-5, 28 %S); **e** — NH$_4$-illite crystals with a lath habit dominating smectite flaky habit (HB-6, 20 %S); **f** — predominantly NH$_4$-illite with lath morphology (HB-7, 10 %S); **g** — lath NH$_4$-illite crystals with straight and pseudo-hexagonal edges (sample HB-7, 10 %S).

Concluding remarks

Our data obtained by SEM and TEM illustrate morphological change during the smectite to illite reaction in a fossil hydrothermal system of Harghita Băi. A long rate of smectite dissolution (around the BPS), illite grown on smectite and a short rate of smectite illitization (in the BPS) were observed. Kaolinite and smectite were two precursor minerals which occurred in the external argillic alteration envelope related to the porphyry copper system. Kaolinite underwent a rapid illitization, before the illitization of smectite took place, as a result of the reaction of kaolinite illitization not being dependent on temperature (Środoń & Eberl 1984).

An attempt has been made to explain whether the type of interlayer cation or the thermodynamic conditions were the main factors influencing the changes of morphology during the illitization of smectite. The type of interlayer cation does not influence the typical morphologies described in the literature along the smectite to illite reaction and therefore, water and pore chemistry played the main role in the illitization process of smectite from Harghita Băi area.

References

Altaner P.S. & Bethke M.C., 1988: Interlayer order in illite/smectite. *Amer. Mineralogist,* 73, 766–774.

Amouric M. & Olives J., 1991: Illitization of smectite as seen by high-resolution transmission electron microscopy. *Eur. J. Mineralogy*, 3, 831–835.

Bobos I., 1994: "Kaolin" deposits of Harghita Mts. Geologic and Metalogenetic study. *Ph.D. Thesis. Department of Mineralogy, "Babes-Bolyai" University of Cluj-Napoca, Romania*, 1–211 (in Romanian).

Bobos I., Šucha V. & Soboleva S.V., 1995: Mixed-layer NH₄-illite/ smectite and NH₄-illite in the hydrothermal area Harghita Bai (East Carpathians). In: Elsen A., Grobet P., Keung M., Leeman H., Schoonheydt R. & Toufar H. (Eds.): *Clays and Clay Materials Sciences. Katholieke University of Leuven, Belgium. Book of Abstracts, Euroclay 95,* 384–385.

Boles J.R. & Franks S.G., 1979: Clay diagenesis in Wilcox sandstones of southwest Texas implications of smectite diagenesis on sandstone cementation. *J. Sed. Petrology*, 49, 55–70.

Buatier M., Peacor D.R. & O Neil J.R., 1992: Smectite-to-illite transition in Barbados accretionary wedge sediments: TEM and AEM evidence for dissolution/crystallisation at low temperature. *Clays and Clay Miner.*, 40, 1, 65–80.

Christidis G., 1995: Mechanism of illitization of bentonites in the geothermal field of Milos island Greece: evidence based on mineralogy, chemistry, particle thickness and morphology. *Clays and Clay Miner.*, 43, 5, 569–585.

Copper J.E. & Abedin K.Z., 1981: The relationship between fixed ammonium-nitrogen and potassium in clays from a deep well on the Texas Gulf Coast. *Texas J. Sci.,* 33, 103–111.

Eberl D.D., Środoń J. & Northrop R.H., 1986: Potasium fixation in

smectite by wetting and drying. In: Davis J.A. & Hays K.F. (Eds.): *Geochemical processes at mineral surfaces. Amer. Chem. Soc. Symp., Ser. 323*, Washington, DC, 296–326.

Eberl D.D. & Środoń J., 1988: Ostwald ripening and interparticle diffraction effects for illite crystals. *Amer. Mineralogist,* 73, 914–934.

Güven M., 1974: Lath-shaped units in fine grained micas and smectites. *Clays and Clay Miner.*, 22, 4, 385–390.

Higashi S., 1978: Dioctahedral mica minerals with ammonium ions. *Miner. J.*, 9, 16–27.

Higashi S., 1982: Tobelite, a new ammonium dioctahedral mica. *Miner. J.,*11, 138–146.

Hower J., Eslinger E.V., Hower M.E. & Perry E.A., 1976: Mechanism of burial metamorphism of argillaceous sediment. *Geol. Soc. Amer. Bull.*, 87, 725–737.

Inoue A., 1986: Morphological change in a continuos smectite-to-illite conversion series by scanning and transmission electron microscopy. *J. Coll. Arts Sci.*, Chiba University, B-19, 23–33.

Inoue A., Kohyama N., Kitagawa R. & Watanabe T., 1987: Chemical and morphological evidence for the conversion of smectite to illite. *Clays and Clay Miner.,* 35, 2, 111–120.

Inoue A.,Velde B., Meunier A. & Touchard G., 1988: Mechanism of illite formation during smectite to illite conversion in a hydrothermal system. *Amer. Mineralogist*, 73, 1325–1334.

Inoue A., Watanabe T., Kohyama N. & Brusewitz A.M., 1990: Characterization of illitization of smectite in bentonite beds at Kinnekule, Sweden. *Clays and Clay Miner.*, 38, 3, 241–249.

Jackson M.L., 1975: Soil chemical analysis-advanced course. *Publ. by author*, Madison, Wisconsin, 1–895.

Jiang W.T. & Peacor D.R., 1990: Transmission and analytical electron microscopy study of mixed-layer illite/smectite formed as apparent replacement product of diagentic illite. *Clays and Clay Miner.*, 38, 5, 449–468.

Kawano M. & Tomita K., 1988: Ammonium bearing dioctahedral 2M₁ mica from Aira district, Kagoshima Prefecture. *Clay Sci.*, 7, 161–169.

Keller W.D., Reynolds R.C. & Inoue A., 1986: Morphology of clay minerals in the smectite-to-illite conversion series by scanning electron microscopy. *Clays and Clay Miner.,* 34, 2, 187–197.

Kozač J., Ocenas D. & Derco J., 1977: Amonna hydrosluda vo Vihorlate. *Miner. slovaca*, 6, 489–494.

Moore D.M. & Reynolds R.C., 1989: X-ray diffraction and the identification and analysis of clay minerals. *Oxford Univ. Press*, 151–153.

Murakami T., Sato T. & Watanabe T., 1993: Microstructure of interstratified illite/smectite at 123 K: A new method for HRTEM examination. *Amer. Mineralogist*, 78, 465–468.

Nadeau P. & Reynolds R.C., 1981: Burial and contact metamorphism in the Mancos Shale. *Clays and Clay Miner.*, 29, 4, 249–259.

Nadeau P., Wilson M.J., McHardy W.J. & Tait J.W., 1985: The conversion of smectite to illite during diagenesis. Evidence from some illitic clays from bentonites and sandstones. *Mineral. Mag.*, 49, 393–400.

Perry E. & Hower J., 1970: Burial diagenesis in Gulf Coast pellitic sediments. *Clays and Clay Miner.,* 42, 114–122.

Roberson H.E. & Lahann W.R., 1981: Smectite to illite conversion rates: effects of solution chemistry. *Clays and Clay Miner.,* 29, 2, 129–135.

Stanciu C., 1984: Hypogene alteration of neogene volcanism of the East Carpathians. *An. Inst. Geol. Geof.,* LXIV, Bucharest, 182–193.

Środoń J., 1980: Precise identification of illite/smectite interstratification by X-ray powder diffraction. *Clays and Clay Miner.*, 28, 5, 401–404.

Środoń J. & Eberl D., 1984: Illite, Mineral. Soc. of Amer., *Rev. Mineralogy*, 495–544.

Šucha V., Kraus I., Gerthofferová H., Peteš J. & Sereková M., 1993: Smectite to illite conversion in bentonites and shales of the East Slovak Basin. *Clay Miner.,* 28, 3, 243–253.

Šucha V., Środoń J., Elsass F. & McHardy W.J., 1996: Particle shape versus coherent scattering domain of illite/smectite: Evidence from HRTEM of Dolná Ves clays. *Clays and Clay Miner.,* 44, 5, 665–671.

Watanabe T., 1988: The structural model of illite/smectite interstratified mineral and the diagram for its identification. *Clay Sci.*, 5, 97–114.

Whitney G. & Northrop H.R., 1988: Experimental investigation of the smectite to illite reaction: Dual reaction mechanism and oxygen-isotope systematics. *Amer. Mineralogist,* 73, 77–90.

Whitney G., 1990: Role of water in the smectite to illite reaction. *Clays and Clay Miner.,* 38, 3, 343–350.

Whitney G. & Velde B., 1993: Changes in particle morphology during illitization: an experimental study. *Clays and Clay Miner.*, 41, 2, 209–218.

Wilson P.N., Parry W.T. & Nash W.P., 1992: Characterization of hydrothermal tobelitic veins from black shale, Oquirrh Mountains, Utah. *Clays and Clay Miner.*, 40, 4, 405–420.

Yau Y.C., Peacor D.R. & McDowell S.D., 1987: Smectite to illite reactions in Salton Sea shales: A transmission and analytical microscopy study. *J. Sed. Petrology*, 57, 335–342.